



Reactive oxygen species dependent degradation pathway of 4-chlorophenol with Fe@Fe₂O₃ core–shell nanowires

Qi Huang, Menghua Cao, Zhihui Ai, Lizhi Zhang*

Key Laboratory of Pesticide & Chemical Biology of Ministry of Education, Institute of Environmental Chemistry, College of Chemistry, Central China Normal University, Wuhan 430079, People's Republic of China

ARTICLE INFO

Article history:

Received 28 March 2014
Received in revised form 24 June 2014
Accepted 26 June 2014
Available online 5 July 2014

Keywords:

Nanoscale zero-valent iron
Molecular oxygen activation
4-Chlorophenol
Diethylenetriaminepentacetate acid
Degradation mechanism

ABSTRACT

In this study, an environmentally benign polyaminocarboxylic ligand diethylenetriamine pentacetate (DTPA) was first used to promote the aerobic 4-chlorophenol (4-CP) degradation with Fe@Fe₂O₃ core–shell nanowires, and then compared with the most used counterpart ethylenediamine tetraacetate (EDTA) of poor biodegradability. Although the 4-CP removal rate in the Fe@Fe₂O₃/DTPA/Air system was slower owing to the preferential degradation of DTPA, the total organic carbon removal rate in the Fe@Fe₂O₃/DTPA/4-CP/Air system was much faster than that in the Fe@Fe₂O₃/EDTA/4-CP/Air system. We interestingly found that hydroxyl radicals could more easily react with DTPA to produce DTPA radicals than with EDTA to produce EDTA radicals. Ligands (DTPA or EDTA) could significantly accelerate the hydroxyl radicals production with Fe@Fe₂O₃, while more hydroxyl radicals were generated in the Fe@Fe₂O₃/DTPA/Air system. We also employed gas chromatography–mass spectrometry and ion chromatography to detect organic intermediates and chloride ions to probe the 4-chlorophenol degradation pathways, and found its degradation pathways were dependent on the reactive oxygen species generated in the different systems. This study can clarify the roles of polyaminocarboxylic ligands on the molecular oxygen activation with nanoscale zero-valent iron, and also provide a green chlorophenols removal method.

© 2014 Elsevier B.V. All rights reserved.

1. Introduction

Chlorophenols are classified as the hazardous and top priority pollutants by the United States Environmental Protection Agency [1,2]. They are chemical intermediates or byproducts in various synthetic industries, and can also be generated during drinking water disinfection process [3,4]. For example, 4-chlorophenol (4-CP) has been widely used in the synthesis of pesticides, herbicides, disinfectants, and wood preservatives. They are irritant to the respiratory and central nervous systems at low levels, and can induce cancer at higher doses. Because of their high toxicity, poor biodegradability, and carcinogenic potential, the removal of chlorophenols is of great significance for environmental protection [5,6].

Advanced oxidation processes (AOPs) could effectively degrade and mineralize chlorophenols via generating highly reactive hydroxyl radicals [7]. However, most of AOPs require the utilization of costly oxidants (ozone and hydrogen peroxide, etc) and/or

intense energy (e.g. ultraviolet light and electricity) [7]. Comparing with ozone and hydrogen peroxide, molecular oxygen is a greener and lower cost oxidant ubiquitously existed in the environment. Unfortunately, the reactions between molecular oxygen and chlorophenols are spin-forbidden at ambient conditions. Therefore, it is a challenge to degrade chlorophenols with activated molecular oxygen.

Iron is the fourth most abundant element in the Earth's crust and therefore involved in many important environmental and biochemical processes, including the generation and consumption of reactive oxygen species (ROS), the decomposition and conversion of organics, as well as the respiration and nutrition intake of some microorganism, and so on. Although the generation of ROS via the reaction of zero-valent iron (ZVI) and molecular oxygen has been reported for many years, the application of iron/oxygen chemistry for environmental pollutant control and remediation is far from satisfactory because of its low ROS generation efficiency. The development of nanotechnology provides a solution to solve this low efficiency problem as scientists have found that the utilization of nanoscale zero-valent iron (nZVI) could enhance the ROS generation to some degree [8]. Fe@Fe₂O₃ core–shell nanowires are a special kind of air stable and highly active nZVI developed by our

* Corresponding author. Tel.: +86 27 6786 7535; fax: +86 27 6786 7535.
E-mail address: zhanglz@mail.ccnu.edu.cn (L. Zhang).

group [9]. Very recently, we found Fe@Fe₂O₃ nanowires showed interesting core-shell structure dependent reactivity on the aerobic 4-CP degradation. However, only 77.8% of 4-CP (1.1 mmol/L) could be aerobically degraded with the most reactive Fe@Fe₂O₃ nanowires in 7 h, accompanying with 30% of mineralization in 10 h. Obviously, further efforts must be made to improve the ROS generation by iron/oxygen chemistry for its practical applications.

It is an important breakthrough for scientists to find that ethylenediamine tetraacetate (EDTA), one of polyaminocarboxylic ligands, could significantly improve the generation of ROS via the reaction of ZVI and molecular oxygen for the degradation of various organic pollutants [10]. Nevertheless, EDTA may cause some unfavorable environmental consequences because of its poor biodegradability and superior heavy metal chelating ability. For example, EDTA may form stable water-soluble complexes with many radionuclides to increase the risk of radionuclide transport in the subsurface environment [11]. It is indispensable to find some safe and environmentally benign replacement for EDTA for the environmental control and remediation purposes. In comparison with EDTA, diethylenetriamine pentaacetate (DTPA) ligand is more environmentally friendly [12–14], but much less been paid attention. In this study, we compare the performances of DTPA and EDTA on the aerobic 4-CP degradation with Fe@Fe₂O₃ nanowires by investigating the generation of ROS as well as the degradation and mineralization of 4-CP systematically. The purposes of this study are to clarify the roles of polyaminocarboxylic ligands on the molecular oxygen activation over nZVI and develop a green method to remove chlorophenols.

2. Experimental

2.1. Chemicals and materials

DTPA, FeCl₃·6H₂O, NaBH₄, TA, and 1,10-phenanthroline monohydrate were all of commercially available analytical grade and purchased from National Medicines Corporation Ltd. of China. 4-CP was purchased from Acros. Superoxide dismutase (SOD), horseradish peroxidase, and *p*-hydroxyphenylacetic acid (POHPAA) were purchased from Aladdin. CH₃OH, C₂H₅OH, C₃H₇OH, and C₄H₉OH were purchased from National Medicines Corporation Ltd. of China. High performance liquid chromatography (HPLC) grade acetonitrile were obtained from Merck. All the chemicals were used as received without further purification. Fe@Fe₂O₃ core-shell nanowires were synthesized by the reaction between ferric chloride and sodium borohydride described previously [15]. Deionized water was used in all experiments.

2.2. Experimental procedure

The aerobic 4-CP degradation experiments were carried out at room temperature (20 ± 2 °C). 4-CP and diethylenetriaminepentaacetic acid were dissolved in aqueous solution. The initial pH of 4-CP and diethylenetriaminepentaacetic acid solution was 2.7. To obtain the same initial pH, the pH of 4-CP and ethylenediamine tetraacetate disodium salt solution was adjusted to 2.7 with 1 mol/L HCl solution. In a typical degradation, Fe@Fe₂O₃ nanowires were added into 4-CP (1.1 mmol/L) and ligand (2 mmol/L) solution with an initial concentration of 0.1 g/L. Air or argon was bubbled into the solution at a rate of 1.5 L/min to continuously supply molecular oxygen or remove molecular oxygen, respectively. During the degradation, the solution samples were taken out from the flask with a syringe at predetermined time intervals and filtered immediately through a 0.22-μm microporous membrane (mixed cellulose esters membrane) for analysis. For comparison, the aerobic 4-CP degradation experiment with 0.1 g/L of Fe@Fe₂O₃ nanowires in the

absence of any polyaminocarboxylic ligand was conducted after adjusting the initial pH of the 4-CP solution to 2.7. The self degradation of 4-CP under air atmosphere and the 4-CP degradation with Fe@Fe₂O₃ and DTPA in argon or oxygen atmosphere were also conducted for comparison.

2.3. Analytic methods

Total organic carbon (TOC) analysis was performed on a TOC analyzer (TOC-V_{CPH}, Shimadzu, Japan) after filtration through 0.22-μm microporous membrane. Methanol, isopropanol, and ethanol were used to probe the generation of •OH in the bulk solution (•OH_{sol}), total hydroxyl radical (•OH_{total}), as well as both •OH and ferryl ions, respectively [8]. Terephthalic acid (TA) was employed as the fluorescent probe for the detection of hydroxyl radicals. 2-hydroxyterephthalic acid (TAOH), which is the fluorescent product of the reaction of TA with •OH, has a strong fluorescent emission at around 426 nm when excited at 312 nm [16]. Electron spin resonance (ESR) spectra were obtained with a Bruker A300 ESR spectrometer with employing 5,5-dimethyl-L-pyrroline-*N*-oxide (DMPO) as the spin trapper at room temperature. Fifty microliter aliquots of control or sample solutions were put into glass capillary tubes with internal diameters of 1 mm and then sealed. The capillary tubes were inserted into the ESR cavity, and the spectra were recorded at selected times. The dissolved ferrous ions was quantified with the 1, 10-phenanthroline method [17]. Samples were analyzed by a UV-vis spectrophotometer (UV-2550, Shimadzu, Japan) at maximum wavelength of 510 nm. Hydrogen peroxide (H₂O₂) was measured by using the horseradish peroxidase-mediated dimerization of POHPAA [18]. The chloride ions and small molecule acids were monitored by an ion chromatographer (Dionex ICS900, Thermo, USA) equipped with IonPac AS14A Anion-Exchange Column. The mobile phase was composed of 8.0 mmol/L Na₂CO₃ and 1.0 mmol/L NaHCO₃. Samples were analyzed at a flow rate of 1 mL/min. The 4-CP concentration was analyzed by high performance liquid chromatography (HPLC, LC-20A, Shimadzu, Japan) with an Agilent TC-C18 reverse phase column (4.6 × 150 mm, 5 μm) and ultraviolet detector setting at the wavelength of 279 nm. The mobile phase was a mixture of acetonitrile and water with 1:1 volume ratio. The injection volume was 10 μL. Samples were analyzed at a flow rate of 0.5 mL/min. The intermediates were analyzed by a gas chromatography-mass spectrometer (GC-MS, Trace 1300-ISQ, Thermo, USA) with Agilent DB-17 capillary column (30 m × 0.25 mm × 0.50 μm). The temperature of the injection block was 300 °C; the oven temperature program was 60 °C, rising at 10 °C/min to a final temperature of 280 °C. Helium was used as the carrier gas at the flow rate of 1 mL/min.

3. Results and discussion

3.1. The removal of 4-CP and TOC

4-CP could not be degraded with air in the absence of Fe@Fe₂O₃, while DTPA or EDTA did not induce the aerobic 4-CP degradation alone. Only 22.3% of 4-CP was aerobically degraded with Fe@Fe₂O₃ in 2 h. The 4-CP removal efficiencies in 2 h reached 100% and 97.3% for the Fe@Fe₂O₃/EDTA/Air and Fe@Fe₂O₃/DTPA/Air systems, respectively (Fig. 1a). The aerobic 4-CP degradation processes were found to follow pseudo-first order kinetics within 90 min (Fig. 1b), while the 4-CP degradation rate constants were 0.0036, 0.0244, and 0.0682 min⁻¹ for the Fe@Fe₂O₃/Air, Fe@Fe₂O₃/DTPA/Air and Fe@Fe₂O₃/EDTA/Air systems, respectively. As expected, the addition of polyaminocarboxylic ligands (EDTA or DTPA) could greatly enhance the aerobic 4-CP degradation with Fe@Fe₂O₃, and the

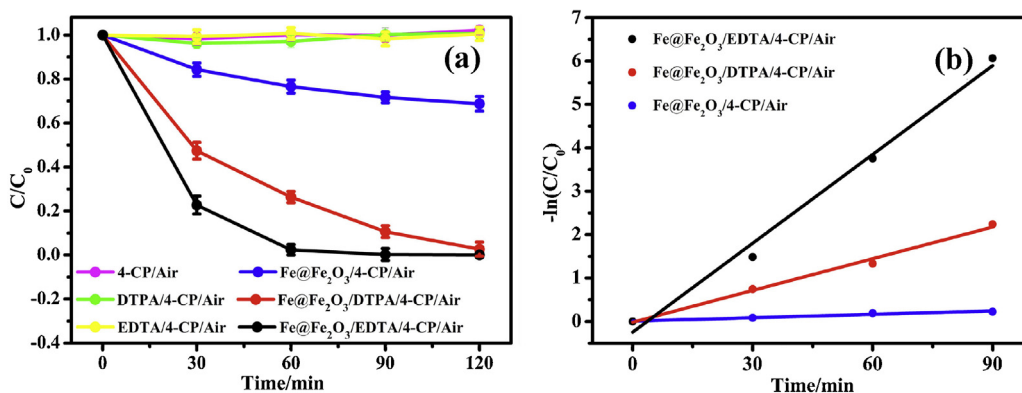


Fig. 1. (a) The temporal concentration changes of 4-CP as a function of time in the 4-CP/Air, DTPA/4-CP/Air, EDTA/4-CP/Air, Fe@Fe₂O₃/4-CP/Air, Fe@Fe₂O₃/DTPA/4-CP/Air, and Fe@Fe₂O₃/EDTA/4-CP/Air systems; (b) plots of $-\ln(C/C_0)$ versus time.

aerobic 4-CP degradation rate in the Fe@Fe₂O₃/EDTA/Air system was nearly 2.8 times that in the Fe@Fe₂O₃/DTPA/Air system within 90 min. However, the TOC removal rate in the Fe@Fe₂O₃/DTPA/4-CP/Air system was 2.4 times that in the Fe@Fe₂O₃/EDTA/4-CP/Air system (Fig. 2a). As both the organic ligands and 4-CP contributed to the TOC values of Fe@Fe₂O₃/ligand/4-CP/Air systems, we therefore monitored the TOC changes in the Fe@Fe₂O₃/DTPA/Air and Fe@Fe₂O₃/EDTA/Air systems without adding 4-CP and found 64.1% of TOC was removed in the Fe@Fe₂O₃/DTPA/Air system within 1 h. This value was much higher than the TOC removal percentage (< 30%) in the Fe@Fe₂O₃/EDTA/Air system (Fig. 2b). Obviously, the 4-CP concentration changes in the Fe@Fe₂O₃/DTPA/4-CP/Air and Fe@Fe₂O₃/EDTA/4-CP/Air systems were different from the

TOC changes. To understand this difference, we further monitored the concentration variation of released chloride ions during the aerobic 4-CP degradation. The dechlorination efficiencies of the Fe@Fe₂O₃/4-CP/Air, Fe@Fe₂O₃/DTPA/4-CP/Air and Fe@Fe₂O₃/EDTA/4-CP/Air systems were 29.8%, 92.5% and 94.1% in 2 h, respectively (Fig. 2c), suggesting that the two ligands (DTPA or EDTA) could significantly enhance the aerobic 4-CP dechlorination with Fe@Fe₂O₃. Therefore, the Fe@Fe₂O₃/DTPA/Air system exhibited lower 4-CP degradation and dechlorination efficiencies than the Fe@Fe₂O₃/EDTA/Air counterpart, but higher TOC removal efficiency. We attributed this inconsistency to the preferential degradation and the faster mineralization rate of DTPA during the simultaneous 4-CP and ligand removal processes.

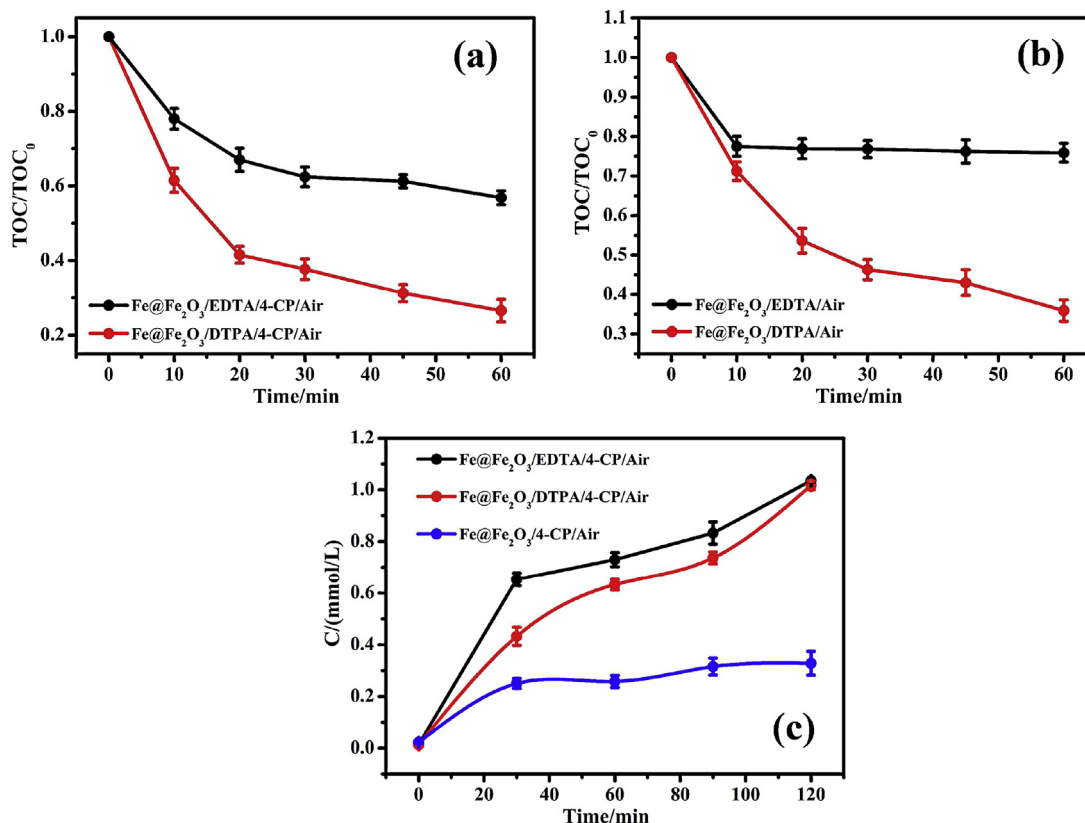


Fig. 2. (a) Normalized TOC changes as a function of time in the Fe@Fe₂O₃/EDTA/4-CP/Air and Fe@Fe₂O₃/DTPA/4-CP/Air systems; (b) normalized TOC changes as a function of time in the Fe@Fe₂O₃/EDTA/Air and Fe@Fe₂O₃/DTPA/Air systems; (c) the concentration variation of chloride ions released during the 4-CP degradation process in the Fe@Fe₂O₃/4-CP/Air, Fe@Fe₂O₃/DTPA/4-CP/Air and Fe@Fe₂O₃/EDTA/4-CP/Air systems.

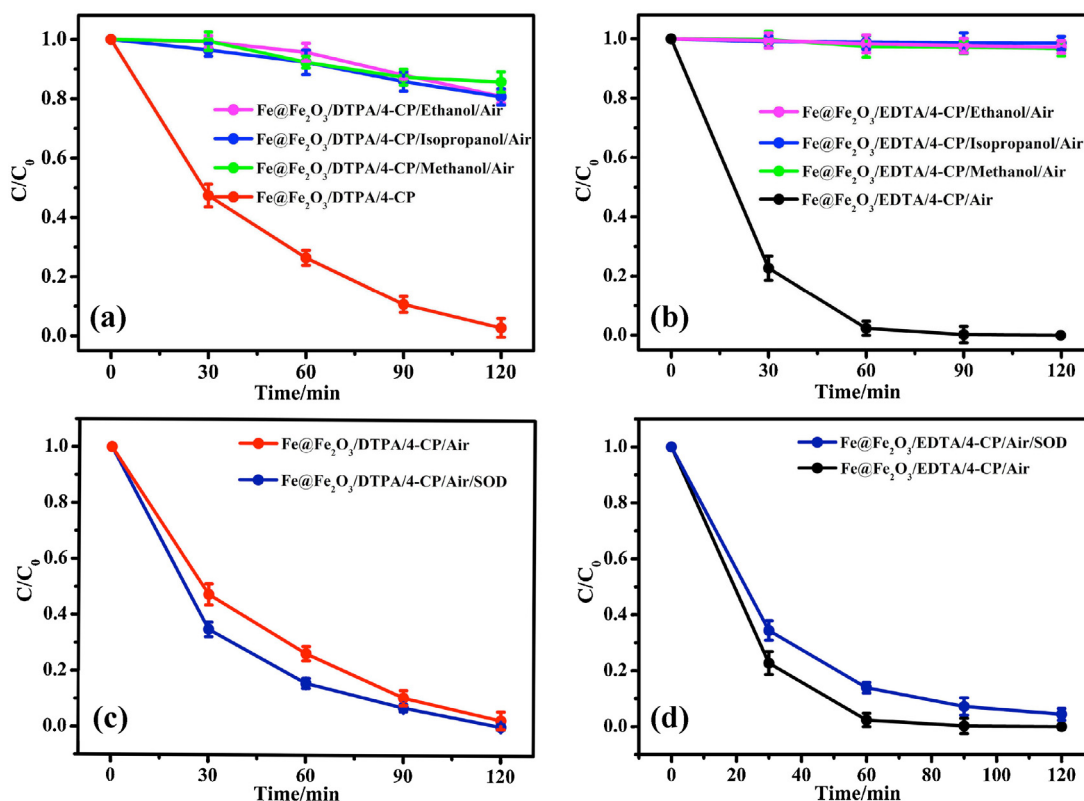


Fig. 3. Degradation of 4-CP in the presence of ethanol, isopropanol, and methanol: (a) the Fe@Fe₂O₃/DTPA/4-CP/Air system; (b) the Fe@Fe₂O₃/EDTA/4-CP/Air system; degradation of 4-CP in the presence of SOD; (c) the Fe@Fe₂O₃/DTPA/4-CP/Air system; (d) the Fe@Fe₂O₃/EDTA/4-CP/Air system.

3.2. The generation and roles of radicals

To clarify the simultaneous 4-CP and ligand removal in the Fe@Fe₂O₃/DTPA/4-CP/Air and Fe@Fe₂O₃/EDTA/4-CP/Air systems, we first analyzed the production of ROS in these two systems with adding different scavengers (ethanol for both •OH and the ferryl ion, isopropanol for total •OH, methanol for •OH in the bulk solution, SOD for •O₂^{•−}). As shown in Fig. 3a and b, the addition of ethanol or isopropanol could largely inhibit the aerobic 4-CP degradation in the two systems with similar inhibition effects. This revealed the major oxidative species for the 4-CP degradation in these two systems were •OH. We also found that the aerobic 4-CP degradation was remarkably inhibited by methanol and therefore concluded that the 4-CP degradation in the two systems was mainly attributed to the •OH in the bulk solution (•OH_{sol}). These •OH_{sol} are thought to be generated by the reaction between diffusing H₂O₂ and Fe(II) (or [Fe(II)-ligand (DTPA or EDTA)]) [19]. Interestingly, we found that •O₂^{•−} played different roles in these two systems, as the 4-CP degradation efficiency increased after the addition of SOD in the Fe@Fe₂O₃/DTPA/4-CP/Air system (Fig. 3c), but decreased in the case of Fe@Fe₂O₃/EDTA/4-CP/Air (Fig. 3d). The SOD induced 4-CP degradation efficiency decrease suggested that •O₂^{•−} might directly contribute to the reductive dechlorination of 4-CP in the Fe@Fe₂O₃/EDTA/4-CP/Air system [9]. We thought that this promotion effect of SOD on the 4-CP degradation efficiency in the Fe@Fe₂O₃/DTPA/4-CP/Air system was related to the SOD promoted transformation of •O₂^{•−} into •OH via the •O₂^{•−} → H₂O₂ → •OH pathway. If •O₂^{•−} did not participate in the 4-CP degradation directly in the Fe@Fe₂O₃/DTPA/4-CP/Air system, its disproportionation into H₂O₂ could be accelerated by SOD [20], resulting in more •OH generation via Fenton reaction for the enhanced 4-CP degradation. We therefore conclude that •O₂^{•−} is directly involved in the reductive

dechlorination of 4-CP in the Fe@Fe₂O₃/EDTA/4-CP/Air system, but indirectly contribute to the oxidative degradation of 4-CP in the Fe@Fe₂O₃/DTPA/4-CP/Air system via its further transformation into •OH.

Recently, we found that the ligand-free aerobic 4-CP degradation with Fe@Fe₂O₃ nanowires was co-governed by two molecular oxygen activation pathways, leading to an interesting core-shell structure dependent reactivity of Fe@Fe₂O₃ nanowires [9]. Among two pathways, one was the two-electron reduction of O₂ to generate H₂O₂ by the Fe⁰, which was realized through the electron transfer from the Fe⁰ core to the surface of iron oxide shell. The other was the one-electron reduction of O₂ to •O₂^{•−} by the surface bound ferrous ions (≡Fe^{III}OFe^{II}OH/≡Fe^{II}OFe^{III}OH). The produced •O₂^{•−} could further react with protons and electrons to produce H₂O₂. All the produced H₂O₂ could then react with the surface bound and dissolved ferrous ions to generate •OH through Fenton reaction. To figure out the roles of ligands (DTPA or EDTA) on the enhanced aerobic 4-CP degradation with Fe@Fe₂O₃ nanowires, we first monitored the concentration variations of Fe(II) in the Fe@Fe₂O₃/Air, Fe@Fe₂O₃/DTPA/Air and Fe@Fe₂O₃/EDTA/Air systems and found that ligands (DTPA or EDTA) could significantly accelerate the release of Fe(II) from iron core of Fe@Fe₂O₃, while more Fe(II) were released in the Fe@Fe₂O₃/DTPA/Air system (Fig. 4). Because the two-electron molecular oxygen reduction process is related with the oxidation of Fe⁰ to ferrous ions and the ligands (DTPA or EDTA) can facilitate the oxidation of Fe(II) to Fe(III) [21], contributing to the one-electron reduction of O₂ to •O₂^{•−}, we proposed that ligands (DTPA or EDTA) might favor both the two-electron and one-electron molecular oxygen reduction processes, which was confirmed by the enhanced H₂O₂ generation with Fe@Fe₂O₃ nanowires in the presence of ligands (Fig. 5). Meanwhile, we also noticed that more H₂O₂ was generated in

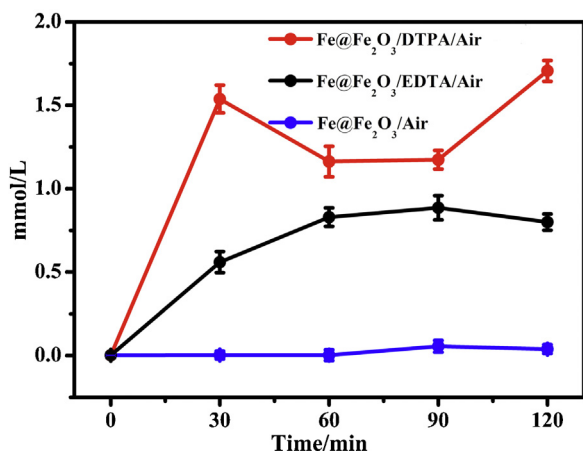


Fig. 4. Comparative concentration of Fe(II) in the Fe@Fe₂O₃/DTPA/Air, Fe@Fe₂O₃/EDTA/Air, and Fe@Fe₂O₃/Air systems.

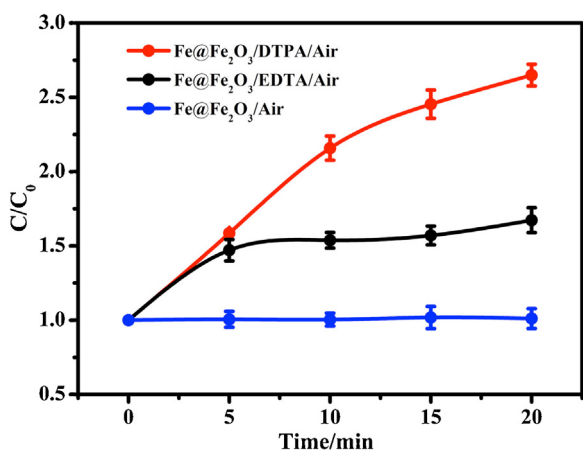


Fig. 5. Comparative production of H₂O₂ in the Fe@Fe₂O₃/DTPA/Air, Fe@Fe₂O₃/EDTA/Air, and Fe@Fe₂O₃/Air systems.

the Fe@Fe₂O₃/DTPA/Air system, suggesting that DTPA was more effective to enhance molecular oxygen activation with Fe@Fe₂O₃ nanowires than EDTA.

It is known that H₂O₂ can react with ferrous ions to produce •OH through Fenton reaction. Spin-trapping ESR technique was therefore employed to identify the short-lived radicals generated in the Fe@Fe₂O₃/EDTA/Air and Fe@Fe₂O₃/DTPA/Air systems. Two

major kinds of radicals were observed in the Fe@Fe₂O₃/EDTA/Air system (Fig. 6a). The poor signal with a ratio of about 1:1:1:1 was assigned to DMPO-•OH [22], and the other stronger ESR signal might be arisen from carbon center radicals like DMPO-•CH₂COOH or DMPO-•EDTA [23–25], which could be produced via the reaction between EDTA and •OH [26]. However, only carbon center radical signal was observed in the typical ESR spectrum of Fe@Fe₂O₃/DTPA/Air system (Fig. 6b). The disappearance of DMPO-•OH signal suggested that all the generated •OH was instantly consumed in the Fe@Fe₂O₃/DTPA/Air system because DTPA was easier to react with •OH to produce DTPA radicals (•DTPA) than EDTA [27], consistent with the environmentally benign characteristic of DTPA.

The TA fluorescent probe method was then used to compare the •OH production in the Fe@Fe₂O₃/Air, Fe@Fe₂O₃/EDTA/Air and Fe@Fe₂O₃/DTPA/Air systems. As ligands (DTPA or EDTA) would compete with TA to react with •OH, and the rate constants of ligands and •OH ($k_{(\bullet\text{OH}+\text{EDTA})} = 2.8 \times 10^9 \text{ L/mol/s}$, $k_{(\bullet\text{OH}+\text{DTPA})} = 5.2 \times 10^9 \text{ L/mol/s}$) had the same order of magnitude as that of TA and •OH ($k_{(\bullet\text{OH}+\text{TA})} = 4.0 \times 10^9 \text{ L/mol/s}$) [27–29], we increased the initial concentration of TA to three orders of magnitude that of ligands (DTPA or EDTA) to get desirable fluorescent signal of 2-hydroxyterephthalic acid, which is produced by the reaction of TA with •OH generated in the systems. Although both DTPA and EDTA could significantly enhance the •OH amount generated via Fe@Fe₂O₃ induced molecular oxygen activation, the •OH generation curve of the Fe@Fe₂O₃/DTPA/Air system was significantly different from that of Fe@Fe₂O₃/EDTA/Air. The amount of 2-hydroxyterephthalic acid in the Fe@Fe₂O₃/EDTA/Air system increased linearly within 120 min (Fig. 7a), suggesting its continuous generation of •OH. As for the Fe@Fe₂O₃/DTPA/Air system, it generated much more 2-hydroxyterephthalic acid than the Fe@Fe₂O₃/EDTA/Air system within the first 30 min (Fig. 7a). Surprisingly, the fluorescent intensity of 2-hydroxyterephthalic acid decreased gradually after 30 min (Fig. 7a), revealing the decomposition of 2-hydroxyterephthalic acid in the Fe@Fe₂O₃/DTPA/Air system. This decomposition might be ascribed to too much •OH produced in the presence of DTPA. The excess •OH would destroy 2-hydroxyterephthalic acid generated via the reaction of TA and •OH. Similar phenomena were also observed previously [30,31]. These •OH measurement results revealed that environmentally benign DTPA was more efficient to enhance molecular oxygen activation with Fe@Fe₂O₃ nanowires than EDTA.

Besides the molecular oxygen activation reactions, zero-valent iron can also reduce proton to hydrogen, which is thought to be a competitive side reaction of molecular oxygen activation [32]. We therefore investigated the influences of two ligands on the

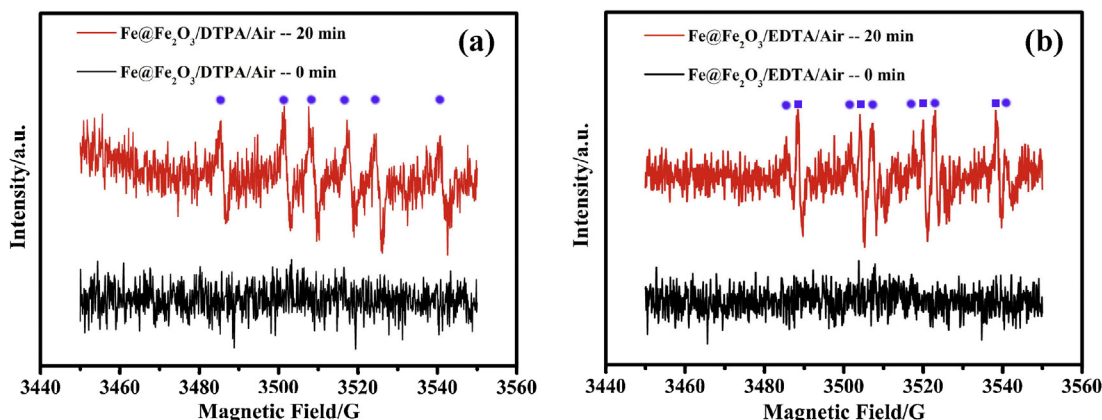


Fig. 6. ESR spectra obtained from samples containing (a) DMPO + Fe@Fe₂O₃ + DTPA; (b) DMPO + Fe@Fe₂O₃ + EDTA at 0 min (black curve) and at 20 min (red curve) under air atmosphere.

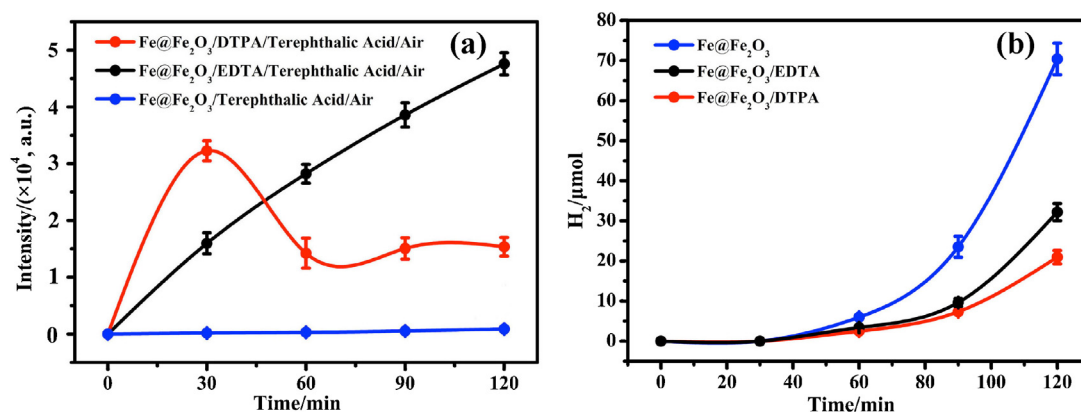


Fig. 7. (a) Time profile of production of 2-hydroxyterephthalic acid in the Fe@Fe₂O₃/Air, Fe@Fe₂O₃/DTPA/Air and Fe@Fe₂O₃/EDTA/Air systems; (b) the temporal production change of H₂ as a function of reaction time.

hydrogen evolution through the reduction of proton by Fe@Fe₂O₃ nanowires. The hydrogen production of the Fe@Fe₂O₃/4-CP/Air, Fe@Fe₂O₃/DTPA/4-CP/Air and Fe@Fe₂O₃/EDTA/4-CP/Air systems were 70.4, 20.9, 32.2 μ mol in 2 h, respectively (Fig. 7b). The results revealed that both DTPA and EDTA inhibited the hydrogen evolution over Fe@Fe₂O₃ nanowires, while DTPA exhibited higher inhibition effect. This phenomenon revealed that DTPA could more effectively suppress the hydrogen evolution through the reduction of proton by Fe@Fe₂O₃ to leave behind more electrons from iron core for the molecular oxygen activation and the subsequent 4-CP degradation.

3.3. The reaction intermediates and pathways

GC–MS analysis was further employed to investigate the 4-CP degradation pathways in the Fe@Fe₂O₃/Air, Fe@Fe₂O₃/EDTA/Air, and Fe@Fe₂O₃/DTPA/Air systems. Both oxidative (hydroquinone) and reductive (phenol) intermediates of 4-CP were detected in the Fe@Fe₂O₃/4-CP/Air system. However, only oxidative intermediates were found in the Fe@Fe₂O₃/EDTA/4-CP/Air and Fe@Fe₂O₃/DTPA/4-CP/Air systems (Fig. 8a and b). This difference indicated that the presence of polyaminocarboxylic ligands could promote the oxidative process during the aerobic 4-CP degradation with Fe@Fe₂O₃ nanowires. Besides hydroquinone detected in the Fe@Fe₂O₃/EDTA/4-CP/Air systems (Fig. 8b), other two oxidative intermediates (4-chlorocatechol and 4-chlororesorcinol) were found in the Fe@Fe₂O₃/DTPA/4-CP/Air system (Fig. 8a), suggesting that the oxidative process was further promoted because of more hydroxyl radicals generated in the system. Ion chromatograph analysis results further confirmed the enhanced 4-CP oxidation in the presence of polyaminocarboxylic ligands. The amount of small molecule acids (e.g. CH₃COOH and HCOOH) generated in the two ligand-existed systems was much more than that in the ligand-free system, while the Fe@Fe₂O₃/DTPA/4-CP/Air system had the highest small molecule acids production (Fig. 9). This was consistent with more hydroxyl radicals generated in the Fe@Fe₂O₃/DTPA/4-CP/Air system than in the other two systems. Obviously, the 4-CP degradation pathways were dependent on the generated reactive oxygen species in this study.

On the basis of the results and analyses, we would explain the reactive oxygen species dependent 4-CP degradation pathways in the three systems as follows. In the absence of polyaminocarboxylic ligands, the amount of generated \bullet OH was tiny, \bullet O₂[−] induced reductive dechlorination of 4-CP was therefore overwhelming, resulting in the phenol generation in the Fe@Fe₂O₃/4-CP/Air

system. The appearance of hydroquinone instead of phenol in the Fe@Fe₂O₃/EDTA/4-CP/Air system reflected the oxidative ability enhancement after adding EDTA. Hydroquinone might be generated in two ways. One was directly via the attack of C–Cl bonds of 4-CP by \bullet OH. The other was indirectly through the further oxidation of phenol (the reductive dechlorination product of 4-CP)

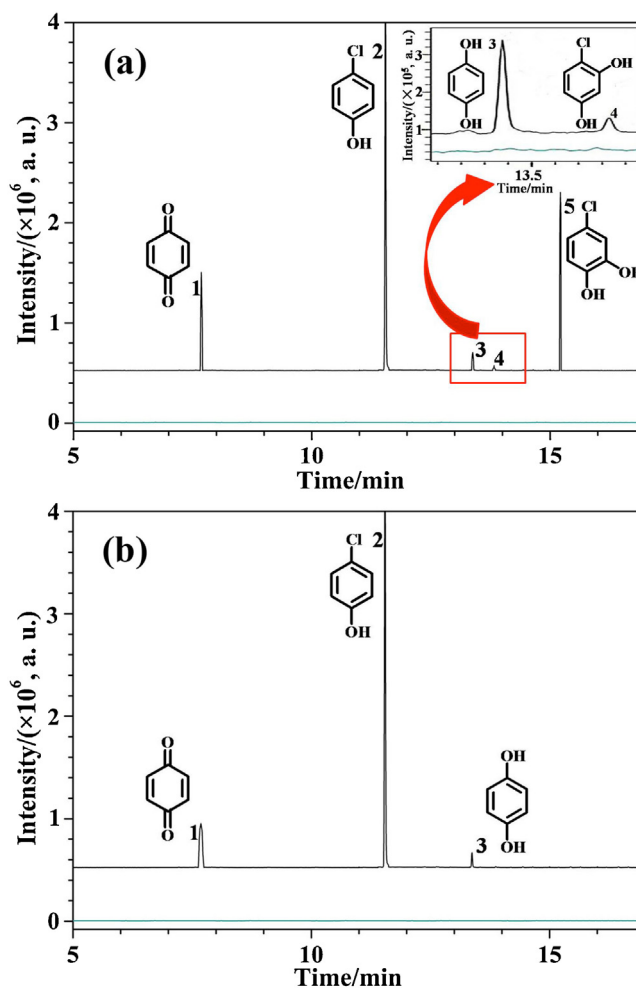


Fig. 8. Typical GC–MS chromatograms for 4-CP degradation: (a) the Fe@Fe₂O₃/DTPA/4-CP/Air system; (b) the Fe@Fe₂O₃/EDTA/4-CP/Air system.

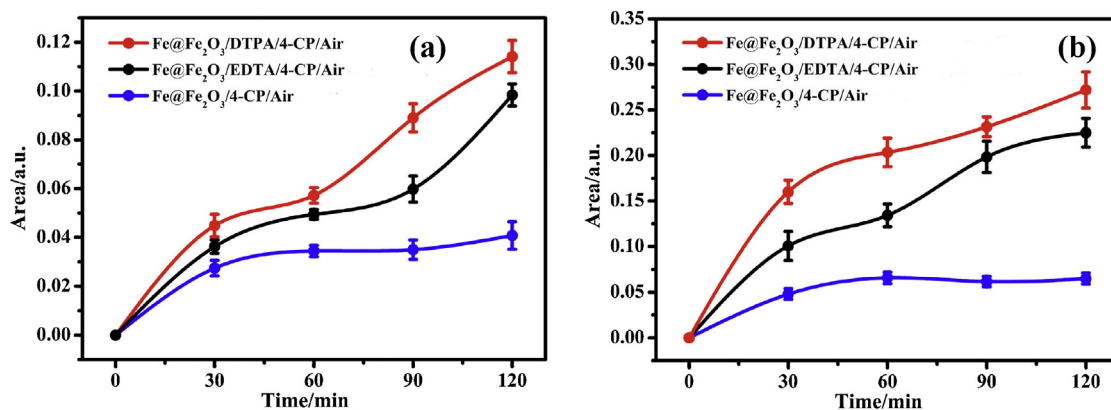
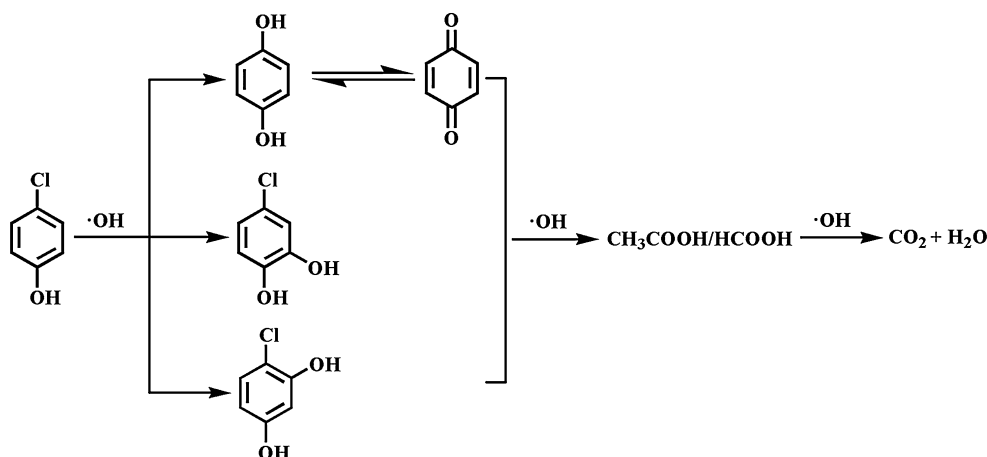
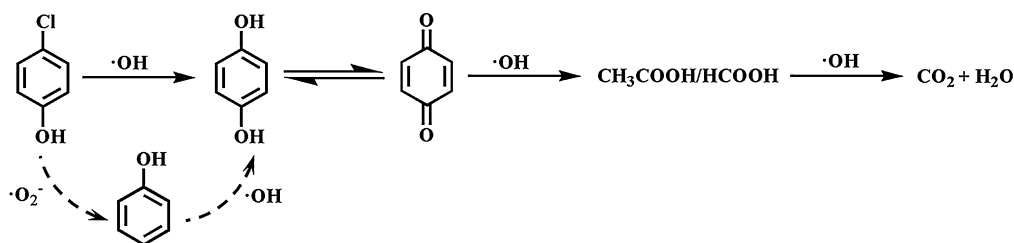


Fig. 9. Comparative production of (a) HCOOH; (b) CH₃COOH in the Fe@Fe₂O₃/4-CP/Air, Fe@Fe₂O₃/EDTA/4-CP/Air and Fe@Fe₂O₃/DTPA/4-CP/Air systems.

(a) In the Fe@Fe₂O₃/DTPA/4-CP/Air System:



(b) In the Fe@Fe₂O₃/EDTA/4-CP/Air System:



Scheme 1. The possible 4-CP degradation mechanisms: (a) the Fe@Fe₂O₃/DTPA/4-CP/Air system; (b) the Fe@Fe₂O₃/EDTA/4-CP/Air system.

with •OH produced in the presence of EDTA (Scheme 1a). As for the Fe@Fe₂O₃/DTPA/Air/4-CP system, it was highly possible that hydroquinone was formed directly through the attack of C–Cl bonds of 4-CP by •OH. This was because •O₂⁻ just indirectly contributed to the 4-CP degradation by its transformation into •OH via •O₂⁻ → H₂O₂ → •OH in the Fe@Fe₂O₃/DTPA/Air/4-CP system, as revealed by the •O₂⁻-trapping experiment results. The other two oxidative intermediates (4-chlorocatechol and 4-chlororesorcinol) were generated via the attack of C–H bonds of 4-CP by •OH because much more •OH was produced in the Fe@Fe₂O₃/DTPA/4-CP/Air system (Scheme 1b). Subsequently, these oxidative and reductive intermediates were further decomposed to small molecule acids (e.g. acetic acid and formic acid), and finally

mineralized into CO₂ and H₂O under the co-attack of •O₂⁻ and •OH.

4. Conclusions

In summary, we have demonstrated that the environmentally friendly diethylenetriamine pentacetate ligand is more effective to promote molecular oxygen activation with Fe@Fe₂O₃ core-shell nanowires than the most used ethylenediamine tetraacetate of poor biodegradable property. Both diethylenetriamine pentacetate ligand and 4-chlorophenol could be rapidly mineralized by more hydroxyl radicals generated through Fe@Fe₂O₃ nanowires induced molecular oxygen activation in the presence of DTPA. We

interestingly found that hydroxyl radicals could more easily react with DTPA to produce DTPA radicals than with EDTA to produce EDTA radicals. The GC–MS and IC detection results revealed that 4-CP degradation pathways were dependent on the reactive oxygen species generated in the different systems. This study can clarify the roles of polyaminocarboxylic ligands on the molecular oxygen activation with nanoscale zero-valent iron, and also provide a green chlorophenols removal method.

Acknowledgements

This work was supported by National Natural Science Foundation of China (Grants 21173093 and 21177048), Key Project of Natural Science Foundation of Hubei Province (Grant 2013CFA114), and self-determined research funds of CCNU from the colleges' basic research and operation of MOE.

References

- [1] T. Ruzgas, J. Emnéus, L. Gorton, G. Marko-Varga, *Anal. Chim. Acta* 311 (1995) 245–253.
- [2] F.X. Ye, D.S. Shen, *Chemosphere* 54 (2004) 1573–1580.
- [3] M.F. Carvalho, I. Vasconcelos, A.T. Bull, P.M.L. Castro, *Appl. Microbiol. Biotechnol.* 57 (2001) 419–426.
- [4] X.H. Xu, D.H. Wang, *Chin. J. Chem. Eng.* 11 (2003) 352–354.
- [5] R. Manimekalai, T. Swaminathan, *Bioprocess Biosyst. Eng.* 22 (2000) 29–33.
- [6] A. Vallecillo, P.A. Garcia-Encina, M. Pena, *Water Sci. Technol.* 40 (1999) 161–168.
- [7] M. Pera-Titus, V. García-Molina, M.A. Banos, J. Giménez, S. Esplugas, *Appl. Catal., B: Environ.* 47 (2004) 219–256.
- [8] C.R. Keenan, D.L. Sedlak, *Environ. Sci. Technol.* 42 (2008) 1262–1267.
- [9] Z.H. Ai, Z.T. Gao, L.Z. Zhang, W.W. He, J.J. Yin, *Environ. Sci. Technol.* 47 (2013) 5344–5352.
- [10] C. Noradoun, M.D. Engelmann, M. McLaughlin, R. Hutcheson, K. Breen, A. Paszczynski, I.F. Cheng, *Ind. Eng. Chem. Res.* 42 (2003) 5024–5030.
- [11] H. Bolton, S.W. Li, D.J. Workman, D.C. Girvin, *J. Environ. Qual.* 22 (1993) 125–132.
- [12] A. Svenson, L. Kaj, H. Björndal, *Chemosphere* 18 (1989) 1805–1808.
- [13] M. Sillanpää, *Chemosphere* 33 (1996) 293–302.
- [14] M. Remberger, A. Svenson, IVL Report No. B, 1256, Swedish Environmental Research Institute, Stockholm, 1997, pp. 53.
- [15] L.R. Lu, Z.H. Ai, J.P. Li, Z. Zheng, Q. Li, L.Z. Zhang, *Cryst. Growth Des.* 7 (2007) 459–464.
- [16] K. Ishibashi, A. Fujishima, T. Watanabe, K. Hashimoto, *J. Photochem. Photobiol., A: Chem.* 134 (2000) 139–142.
- [17] W.B. Fortune, M.G. Mellon, *Ind. Eng. Chem. Anal. Ed.* 10 (1938) 60–64.
- [18] A.L. Lazrus, G.L. Kok, S.N. Gitlin, J.A. Lind, S.E. McLaren, *Anal. Chem.* 57 (1985) 917–922.
- [19] S.H. Joo, A.J. Feitz, D.L. Sedlak, T.D. Waite, *Environ. Sci. Technol.* 39 (2005) 1263–1268.
- [20] A.J. Kettle, R.F. Anderson, M.B. Hampton, C.C. Winterbourn, *Biochemistry* 46 (2007) 4888–4897.
- [21] V. Zang, R. Van Eldik, *Inorg. Chem.* 29 (1990) 1705–1711.
- [22] W.J. Li, D.Z. Li, J.J. Xian, W. Chen, Y. Hu, Y. Shao, X.Z. Fu, *J. Phys. Chem. C* 114 (2010) 21482–21492.
- [23] S.J. Klebanoff, A.M. Waltersdorph, B.R. Michel, H. Rosen, *J. Biol. Chem.* 264 (1989) 19765–19771.
- [24] Z.H. Wang, X. Chen, H.W. Ji, W.H. Ma, C.C. Chen, J.C. Zhao, *Environ. Sci. Technol.* 44 (2009) 263–268.
- [25] B.C. Gilbert, G.R. Hodges, J.R.L. Smith, P. MacFaul, P. Taylor, *J. Chem. Soc., Perkin Trans. 1* 2 (1996) 519–524.
- [26] P.S. Surdhar, D.A. Armstrong, K.H. Schmidt, W. Mulac, *Int. J. Radiat. App. Instr., C Radiat. Phys. Chem.* 32 (1988) 15–21.
- [27] D.E. Cabelli, J.D. Rush, M.J. Thomas, B.H.J. Bielski, *J. Phys. Chem.* 93 (1989) 3579–3586.
- [28] S.N. Bhattacharyya, K.P. Kundu, *Int. J. Radiat. Phys. Chem.* 4 (1972) 31–41.
- [29] T. Charbouillot, M. Brigante, G. Mailhot, P.R. Maddigapu, C. Minero, D. Vione, *J. Photochem. Photobiol., A: Chem.* 222 (2011) 70–76.
- [30] K.C. Pillai, T.O. Kwon, I.S. Moon, *Appl. Catal., B: Environ.* 91 (2009) 319–328.
- [31] R. Thiruvengatachari, T.O. Kwon, J.C. Jun, S. Balaji, M. Matheswaran, I.S. Moon, *J. Hazard. Mater.* 142 (2007) 308–314.
- [32] L. Wang, M.H. Cao, Z.H. Ai, L.Z. Zhang, *Environ. Sci. Technol.* 48 (2014) 3354–3362.